

Quantum Imaging and Metrology with Undetected squeezed Photons: Noise Canceling and Noise Based Imaging

Saheb Samimi and Zahra Ghasemi

*Faculty of Physics, University of Isfahan, Hezar Jarib, 81746-73441, Isfahan, Iran and
Center of Quantum Science and Technology (CQST),
University of Isfahan, Hezar Jarib, Isfahan, Iran*

Hamidreza Mohammadi *

*Faculty of Physics, University of Isfahan, Hezar Jarib, 81746-73441, Isfahan, Iran
Quantum Optics Group, Faculty of Physics, University of Isfahan, Hezar Jarib, Isfahan, Iran and
Center of Quantum Science and Technology (CQST),
University of Isfahan, Hezar Jarib, Isfahan, Iran
(Dated: November 11, 2024)*

In this work a quantum imaging setup based on undetected squeezed photons is employed for metrological applications such as sensitive phase measurement and quantum imaging. In spite of the traditional quantum imaging with undetected photons, introduced by A. Zeilinger *et. al*, the proposed setup is equipped by a homodyne detection and also the brightness of the quantum light is enhanced by an optical parametric oscillator (OPO). Introducing OPO may be diminish the validity of the low gain approximation, so a theoretical approach beyond this approximation is introduced. Due to the resource of squeezing, the results reveal the higher amount of signal to noise ratio, as a measure of image quality and phase-measurement accuracy. Accordingly, an imaging protocol is introduced to suppress the background noises, effectively. Interestingly, This protocol provides a way to extract the image information which is encoded in the quantum fluctuation (noise). Therefore, non-disruptive imaging is achievable, which is noteworthy subject in the field of bio-imaging of sensitive and low damage threshold living cells.

I. INTRODUCTION

Interferometry provides a powerful technique to measure physical quantities with high precision and sensitivity[1]. In the conventional interferometers the sensitivity is bounded by Shot-Noise-Limit (SNL)[2–4]. The ultimate goal in the interferometry is to overcome SNL. Non-classical properties of lights may provide an effective resources to gain this purpose[5–15]. In recent years, along with development of non-linear optical process, the optical non-linear interferometry attracted extensive attentions, to realize interferometer with strong sensitivity and accuracy [16–19]. SU(1,1) interferometers are almost the most important non-linear interferometer due to their sensitivity enhancement[16, 20–26]. These interferometers are used in direct detection of gravitational waves[25].

In the SU(1,1) interferometer, the beam splitters of conventional interferometer are replaced by a two-mode squeezer apparatuses such as Optical Parametric Amplifiers(OPAs)[27]. In the devices, which are using non-degenerate SU(1,1) interferometer, the interaction and detection often applied in different wavelength[28–30]. In the other word, these type of device can provide two mode squeezed light with different wavelength called signal and idler beams. Operating in two non-degenerate wavelength makes SU(1,1) interferometer to become powerful devices in quantum metrology such as

spectroscopy[31, 32], imaging[33, 34] and optical coherent tomography(OCT)[2, 35]. This properties have significant application in image construction of biological molecules and living cells[36, 37] because the interaction could be occur in mid-infrared and detection is applied in the optical spectrum[38].

Quantum Imaging with Undetected Photon (QUIP) is an imaging protocol in which SU(1,1) interferometer is used in image formation such that the idler beam interacts with an object while detection of the object achieved by signal beam which never interacts with the object[30]. This type of imaging is developed by Anton Zeilinger *et al.*[39]. In their setup, a pair signal and idler beam are generated by Spontaneous Emission Down Conversion (SPDC)process in a non-linear crystal. The idler beam guided to the second non-linear crystal after interacting with the object. In the second non-linear crystal a new signal and idler pair are created. The signal generated by the first and second non-linear crystals interfere to form the image. The construction and deconstruction patterns appears due to the path indistinguishability which is related to the quantum nature of the light[40]. The quantum theory of QUIP is developed by Mayukh Lahiri *et al.* in Ref.[41]. In this research the low gain regime is used to model wave mixing in the non-linear crystals. The resolution of QUIP is studied in near-field and far-field imaging using Gaussian beam profiles[42]. In the near-field imaging the minimum resolvable distance between two point sources is determined by Point Spread Function (SPF) width which is proportional to the square root of crystal length[43], while in the far-field QUIP res-

* hr.mohammadi@sci.ui.ac.ir

olution is independent to the length of the non-linear crystals[43]. Moreover QUIP protocol is implemented in the microscopy[44] and holography devices[45].

However, since in the theoretical treatment of QUIP the low gain approximation is used, the results cannot be applied to the setup for those the low gain approximation is invalid. In this paper we present the theoretical treatment of QUIP beyond low gain approximation. To this end, it assumed that the non-linear crystals are derived by *classical pump beam*. Since in the present theoretical description the low gain approximation is ignored, it is applicable to the QUIP with desired gain regime. It is also, we introduce an imaging protocol in which one can suppress the background noises. The novel scheme is the image construction from a low damage threshold object which is known as Quadrature-Noise Shadow Imaging (QSI). This scheme is based on quadrature quantum noise measurement[46]. QSI allows to image with low photons number. Moreover, in the QSI the detrimental dark count noise of the sensor is eliminated in the real setups [46–48]. Interestingly, we found that the image information is also coded into the noise by which the image may reconstructed using QSI.

This paper is organized as follow: In the next section the setup under consideration is described. Section III is devoted to the theoretical description of the model. In first subsection of Sec.IV the object low transmittivity is characterized while in second subsection the high transmittivity is addressed. Accordingly two imaging protocols are introduced in Sec. V. Finally the conclusion and remarks of this work are provided in Sec. VI.

II. PROPOSED SETUP

In this section we demonstrate the proposed setup. The schematic diagram of the setup is depicted in figure 1. The image reconstruction is shown in figure 1 through four stages. In the first stage the two mode squeezed state beams are generated via a non-degenerated Optical Parametric Oscillator (NONPO), constructed by a non-linear crystal ($\chi_1^{(2)} \neq 0$) implemented in the center of a confocal cavity. Then each squeezed mode (output of coupler M_2) is separated to signal and idler mode by a dichoric mirror, DM . The signal (green) beam arrives to the second non-linear crystal ($\chi_2^{(2)} \neq 0$) and the idler (red) beam is reflected through DM toward the object. The idler interacts with an object modeled by a lossless beam splitter with transmission $Te^{i\phi_T}$ (reflection $Re^{i\phi_R}$). In order to provide path identity, a portion of the idler, which is transmitted through the object, is combined with the idler beam generated in the second non-linear crystal. The information about the object is transferred from idlers to signals beam due to the three wave mixing phenomenon which occurs in the 2nd crystal, $\chi_2^{(2)}$. Finally, since the object information are encoded in the signal quadrature, a balance homodyne de-

tection is applied to the outcome signal of the second non-linear crystal to extract the image information. It is worth noting that undetected light refers to the idler beam as no measurement applied to it.

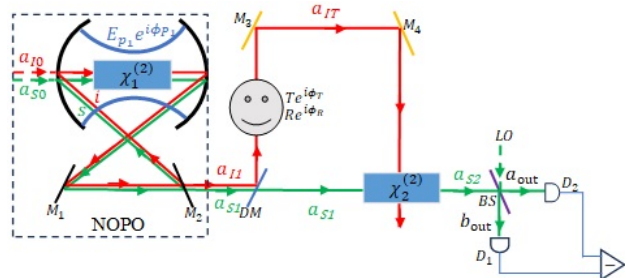


FIG. 1. Schematic diagram of the setup

In the following section we provide a theoretical description of how the image information extracted.

III. THEORETICAL DESCRIPTION OF THE MODEL

In this section we present theoretical description about image formation. As shown in figure 1, the output electrical signal of the balanced homodyne detection can be calculated as:

$$S = \frac{1}{4}\beta \left(a_{S2}^\dagger e^{-i\phi_\beta} + a_{S2} e^{i\phi_\beta} \right), \quad (1)$$

where we assumed that the local oscillator in the homodyne detection is prepared in coherent state $|\beta e^{i\phi_\beta}\rangle$. The annihilation (creation) operator a_{S2} (a_{S2}^\dagger) is correspond to the output signal beam from second non-linear crystal. As mentioned in the previous section, the object information is encoded into beam, $S2$. So, the aim is to relate a_{S2} to the initial condition and object properties. To this end we assume that NONPO is derived by classical field with fixed phase, ϕ_{P1} . The classical pump field implies the wave mixing process in the first non-linear crystal, $\chi_1^{(2)}$. Since the squeezing occurs via parametric down conversion process, the output of NONPO becomes,

$$a_{S1} = G_1 a_{S0} + g_1 e^{i\phi_{P1}} a_{I0}^\dagger, \quad (2a)$$

$$a_{I1} = G_1 a_{I0} + g_1 e^{i\phi_{P1}} a_{S0}^\dagger, \quad (2b)$$

where the input signal and idler annihilation (creation) operators are denote by a_{S0} (a_{S0}^\dagger) and a_{I0} (a_{I0}^\dagger), respectively. In Eqs. (2) the squeezing process is characterized by G_1 and g_1 . As mentioned above, the object is characterized as a lossless beam splitter. Therefore the transmitted idler field is given by,

$$a_{IT} = Te^{i\phi_T} a_{I1} + Re^{i\phi_R} a_{IL}. \quad (3)$$

In this equation, the input field to empty port of the beam splitter (object) is denoted by a_{IL} . Using Eq. (2b) in (3), gives

$$a_{IT} = T e^{i\phi_T} \left(G_1 a_{I0} + g_1 e^{i\phi_{P1}} a_{S0}^\dagger \right) + R e^{i\phi_R} a_{IL}. \quad (4)$$

Since two beams (a_{S1} and a_{IT}) are mixed in the second non-linear crystal and gives rise to built up beam S_2 , we have,

$$a_{S2} = G_2 a_{S1} + g_2 e^{i\phi_{P2}} a_{IT}^\dagger, \quad (5)$$

where the non-linear (squeezing) process in the second crystal is characterized by G_2 , g_2 and ϕ_{P2} is the phase of classical field which pumps the second wave mixing process. Substituting Eqs. (2a) and (4) into Eq. (5) leads to,

$$a_{S2} = G a_{S0} + g a_{I0}^\dagger + r a_{IL}^\dagger. \quad (6)$$

where $G = G_1 G_2 + g_1 g_2 T \exp(i\phi_1)$, $g = g_1 G_2 \exp(i\phi_{P1}) + G_1 g_2 T \exp(i\phi_2)$ and $r = g_2 R \exp(i\phi_3)$. In the expression for G , g and r the definitions $\phi_1 = \phi_{P2} - \phi_{P1} - \phi_T$, $\phi_2 = \phi_{P2} - \phi_T$ and $\phi_3 = \phi_{P2} - \phi_R$ are used. It is worth noting, since $|G|^2 - |g|^2 - |r|^2 = 1$ is satisfied, the commutation relation $[a_{S2}, a_{S2}^\dagger] = 1$ is also preserved.

IV. DESCRIPTION CHARACTERISTIC OF THE SYSTEM

In this section we describe behavior of the system. To this end we assumed that the input signal beam is in coherent state $|\alpha e^{i\phi_\alpha}\rangle$ and all other modes are in the vacuum state. Hence the mean value of S with respect to $(|\Psi\rangle = |\alpha e^{i\phi_\alpha}\rangle_{S0} |0\rangle_{I0} |0\rangle_{IL})$ is as given by:

$$\langle S(\delta, \Delta) \rangle = 2\alpha\beta |G| \cos(\phi_G(\Delta) + \delta), \quad (7)$$

where, $\delta = \phi_\alpha + \phi_\beta$, $\Delta = \phi_{P2} - \phi_{P1}$ and ϕ_G is defined as,

$$\phi_G(\Delta) = \tan^{-1} \left(\frac{x \sin(\Delta - \phi_T)}{1 + x \cos(\Delta - \phi_T)} \right), \quad (8)$$

where $x = T g_1 g_2 (G_1 G_2)^{-1}$. Since g_i and G_i ($i = 1, 2$) are correspond to the parametric process gains and $T \leq 1$, the condition $0 \leq x \leq 1$ is satisfied. In Eq. (7), $|G|$ is,

$$|G(\Delta)|^2 = G_1^2 G_2^2 [x^2 + 2x \cos(\Delta - \phi_T) + 1]. \quad (9)$$

The signal-to-noise ratio (SNR) has a crucial role in sensing include imaging. In this section we calculate noise term of the system which arises from quantum fluctuations. To this end we need to calculate $\langle \Delta S^2 \rangle_\Psi = \langle \Psi | S^2 | \Psi \rangle$. Hence the uncertainty in signal measurement is given by,

$$\langle \Delta S^2 \rangle = \beta^2 (2|G|^2 - 1). \quad (10)$$

Interestingly, the quantum uncertainty given by Eq. (10) is related to the optical properties of the object through G parameter. Therefore, the image can be also reconstructed using quantum noise (see section V A). The SNR (defined by $\langle S \rangle^2 / \langle \Delta S^2 \rangle$) can be calculated as:

$$\text{SNR} = 4\alpha^2 \Gamma \cos^2(\phi_G + \delta). \quad (11)$$

Here the factor Γ is defined as $\Gamma = |G|^2 (2|G|^2 - 1)^{-1}$. Since $|G|^2 = 1 + |g|^2 + |r|^2 \geq 1$ is satisfied (see Sec. II), Γ has a finite value.

In the following for better illustration, the spacial limits $x \rightarrow 0$ (opaque object) and $x \rightarrow 1$ (transparent object) are demonstrated, separately.

A. The Limit $x \rightarrow 0$

For an object with low transmission co-efficient the condition $x \rightarrow 0$ is satisfied. In this case, $|G|$ tends to $G_1 G_2$ and $\phi_G \approx x \sin(\Delta - \phi_T)$. Substituting these results in Eq. (7) and ignoring $O(x^3)$ and higher terms, one finds,

$$\langle S \rangle \approx 2\alpha\beta G_1 G_2 \left(\cos \delta - \phi_G \sin \delta - \frac{1}{2} \phi_G^2 \cos \delta \right). \quad (12)$$

The small change in ϕ_T leads to the variation in the output signal as follows,

$$|\delta \langle S \rangle| = 2\alpha\beta G_1 G_2 \left| (\sin \delta + \phi_G \cos \delta) \frac{d\phi_G}{d\phi_T} \right| \delta \phi_T. \quad (13)$$

For the leading purposes, we investigate the last equation for $\delta = k\pi/2$, where k is an integer number.

$$|\delta \langle S \rangle| = \begin{cases} 2x\alpha\beta G_1 G_2 |\cos(\Delta - \phi_T)| \delta \phi_T & k \text{ is odd} \\ x^2 \alpha\beta G_1 G_2 |\sin 2(\Delta - \phi_T)| \delta \phi_T & k \text{ is even} \end{cases}. \quad (14)$$

This equation reveals that, for an object with low transmission, the small change in the phase leads to a change in output signal which is proportional to $G_1 G_2$. Therefore sensitivity of a fixed system can be enhanced by non-linear process gains which is depend on tunable parameters such as the phase and amplitude of the pump field. From this equation, it is also concluded that behavior of the system is depend on selection of k number such that for the odd values of k , output signal related on x while for an even value, this quantity is proportional to x^2 . In the limit of $x \rightarrow 0$, Eq. (11) becomes,

$$\text{SNR} = \begin{cases} 4\alpha^2 \Gamma \phi_G^2 & k \text{ is odd} \\ 4\alpha^2 \Gamma & k \text{ is even} \end{cases}, \quad (15)$$

where, $\lim_{x \rightarrow 0} \Gamma = G_1 G_2 (2G_1 G_2 - 1)^{-1}$. In the low and high gain regime Γ approaches to 1 and 0.5, respectively.

Finally, from Eq. (14), one can conclude that SNR depend on x^2 for odd values of k while for even values SNR is independent of x . Eq. (15) implies that SNR can be improved by adjusting the mean photon number in the input signal field of NOPO.

B. The Limit $x \rightarrow 1$

The limit $x \rightarrow 1$ is achieved in high gain regime and high transmission. In this regime $\phi_G = (\Delta - \phi_T)/2$ and Eq.(9) takes form,

$$|G| = 2G_1G_2 \left| \cos\left(\frac{\Delta - \phi_T}{2}\right) \right|. \quad (16)$$

Substituting (16) into (7) and differentiating the resulted equation with respect to ϕ_T leads to,

$$|\delta \langle S \rangle| = \begin{cases} 2\alpha\beta G_1G_2 |\cos(\Delta - \phi_T)| \delta\phi_T & k \text{ is odd} \\ 2\alpha\beta G_1G_2 |\sin(\Delta - \phi_T)| \delta\phi_T & k \text{ is even.} \end{cases} \quad (17)$$

It is worth mentioning that in Eq. (17), we take $\delta = k\pi/2$. The sensitivity given by Eq. (17) is independent of x and proportional to the factor G_1G_2 . We substitute (16) and its corresponding ϕ_G in Eq.(11) to obtain SNR,

$$\text{SNR} = \begin{cases} 2\alpha^2 \sin^2\left(\frac{\Delta - \phi_T}{2}\right) & k \text{ is odd} \\ 2\alpha^2 \cos^2\left(\frac{\Delta - \phi_T}{2}\right) & k \text{ is even.} \end{cases} \quad (18)$$

Since Eq.(18) depend on adjustable parameter α , SNR one can improve it by increasing the mean photon numbers in input signal field of NOPO.

V. IMAGING PROTOCOL

This section is devoted to how construct the image using either of quantum fluctuation or signal. In the following subsection we present a protocol to extract object information by quantum fluctuation. Also the image construction protocol using the homodyne signal is the subject of subsection V B

A. Imaging Protocol Using Quantum Fluctuation

Since the quantum fluctuation (noise term) depends on the parameter G (see Eq. (10)), which contains the object information, we can construct the image using the quantum fluctuation. To this end we use Eq.(9) to rewrite Eq.(10) as follows,

$$\frac{1}{2G_1^2G_2^2} \left[1 + \frac{\langle \Delta S^2(\Delta) \rangle}{\beta^2} \right] = 1 + x^2 + 2x \cos(\Delta - \phi_T). \quad (19)$$

It is worthwhile to emphasis that Δ is experimentally adjustable parameter via precise tuning the phase mismatch of the classical fields pumping the crystals, see figure 1. Therefore the image construction processes can be achieved by the following protocol:

- i) At first stage, the values of $\langle \Delta S^2(\Delta) \rangle$ for $\Delta = 0, \pi/2, 3\pi/2, \pi$ is measured.
- ii) The 2nd stage is to calculate the image information by the following formulas:

$$T = \frac{\sqrt{[\langle \Delta S^2(0) \rangle - \langle \Delta S^2(\pi) \rangle]^2 + [\langle \Delta S^2(\frac{\pi}{2}) \rangle - \langle \Delta S^2(\frac{3\pi}{2}) \rangle]^2}}{4\beta^2 g_1 g_2 G_1 G_2}, \quad (20)$$

and

$$\phi_T = \tan^{-1} \left(\frac{\langle \Delta S^2(\frac{\pi}{2}) \rangle - \langle \Delta S^2(\frac{3\pi}{2}) \rangle}{\langle \Delta S^2(0) \rangle - \langle \Delta S^2(\pi) \rangle} \right). \quad (21)$$

B. Imaging Protocol using Signal

Similarly, the image information (T and ϕ_T) can be extracted by the output signal. The signal measured by homodyne detection is governed by Eq. (7) which is proportional to $|G|$. Fortunately, $|G|$ is a function of two experimentally adjustable parameters, δ and Δ . Hence the following protocol is experimentally executable:

- i) Fixing the values $\delta = 0, \pi/2$. Under these conditions, the signals measured by detector $\langle S(\delta, \Delta) \rangle$ can be expressed as:

$$\langle S(0, \Delta) \rangle = 2\alpha\beta |G| \cos \phi_G, \quad (22a)$$

$$\langle S\left(\frac{\pi}{2}, \Delta\right) \rangle = -2\alpha\beta |G| \sin \phi_G. \quad (22b)$$

Where,

$$|G(\Delta)|^2 = \frac{\langle S(0, \Delta) \rangle^2 + \langle S(\frac{\pi}{2}, \Delta) \rangle^2}{4\alpha^2\beta^2}. \quad (23)$$

- ii) Using the fact that Δ (pumps phase mismatch) is also an adjustable parameter we set $\Delta = 0, \pi/2, \pi, 3\pi/2, \pi$ in Eq. (11) and use results to obtain the information about object,

$$T = \frac{(|G(\pi/2)|^2 - |G(3\pi/2)|^2)^2 + (|G(0)|^2 - |G(\pi)|^2)^2}{4G_1G_2g_1g_2}. \quad (24)$$

and

$$\phi_T = \tan^{-1} \left[\frac{|G(\pi/2)|^2 - |G(3\pi/2)|^2}{|G(0)|^2 - |G(\pi)|^2} \right], \quad (25)$$

According to Eq.(23), T and ϕ_T are functions of $\langle S(0, 0) \rangle$, $\langle S(\pi/2, 0) \rangle$, $\langle S(0, \pi/2) \rangle$, $\langle S(\pi/2, \pi/2) \rangle$, $\langle S(0, \pi) \rangle$, $\langle S(\pi/2, \pi) \rangle$, $\langle S(0, 3\pi/2) \rangle$, $\langle S(\pi/2, 3\pi/2) \rangle$. We

emphasize that, although, Eq. (9) consist of background noises (see the first two term of Eq. (9)), The last two equations are noise-free. Note that the noise terms in Eq. (25) and the numerator of Eq. (24) are canceled through the calculation, thanks to the homodyne detection.

VI. SUMMARY AND CONCLUSION

In the present work an imaging setup is considered. In the proposed setup a classical pump field excites a non-linear crystal posses second order susceptibility, $\chi_1^{(2)} \neq 0$, to produce non-degenerate squeezed photon pair (called signal and idler) which is aligned on the center of a confocal cavity to construct a non-degenerate optical parametric oscillator (NOPO). The NOPO is pumped by a coherent light and stimulated by a input coherent beam prepared in the signal frequency. The output idler beam emerging from NOPO interacts with the object and then injected into a second non-linear crystal, same to the first crystal. This idler beam merges with idler beam generated in the second crystal during SPDC process, in order to achieve path identity. The image information can be extracted by a balanced homodyne detection of the signal beam emerged from NOPO and signal beam generated by the SPDC process in the second crystal. Notice that, these signal beams never interacts with the object. Along with the theoretical treatment of the setup, the quantum fluctuation is also calculated. Interestingly, we found that the image information (transition coefficient

and phase) can be also extracted from quantum fluctuation. Our calculations show that SNR is enhanced as a function of the photon mean number of input signal field. The further theoretical calculation is applied for both oblique object ($x \rightarrow 0$) and transparent object ($x \rightarrow 1$) cases.

For the first regime ($x \rightarrow 0$) the behavior of SNR strongly depends on the relative phase of the input signal field to the NOPO and homodyne local oscillator. In this regime, at the high and low parametric gains, SNRs are scaled by 0.5 and 1 respectively. The second regime occurs at high parametric gain and high object transmission ($x \rightarrow 1$). In this regime, SNR is independent of parametric gains.

Finally we presented an imaging protocol to remove classical background noises. In this protocol, the output electric signals from the balanced homodyne setup are measured after adjusting phases ϕ_α , ϕ_β and the pumps phases as described in Sec.V. In this way, the image information can be superimposed on the homodyne signal, where background noises are suppressed. The noiseless image information (such as object transmission and phase) can be extracted from the signals which are measured by the balanced homodyne setup.

In view of the aforementioned point the results of the present work provide effective theoretical treatment to optimize SNR in the QUIP. Moreover the proposed setup and the presented imaging protocol lead to QUIP without background noises.

-
- [1] G. Frascella, E. Mikhailov, N. Takanashi, R. Zakharov, O. Tikhonova, and M. Chekhova, Wide-field su (1, 1) interferometer, *Optica* **6**, 1233 (2019).
 - [2] Y. Gao, Quantum optical metrology in the lossy su(2) and su(1,1) interferometers, *Phys. Rev. A* **94**, 023834 (2016).
 - [3] C. M. Caves, Quantum-mechanical noise in an interferometer, *Phys. Rev. D* **23**, 1693 (1981).
 - [4] M. Takeoka, K. P. Seshadreesan, C. You, S. Izumi, and J. P. Dowling, Fundamental precision limit of a mach-zehnder interferometric sensor when one of the inputs is the vacuum, *Phys. Rev. A* **96**, 052118 (2017).
 - [5] R. Carranza and C. C. Gerry, Photon-subtracted two-mode squeezed vacuum states and applications to quantum optical interferometry, *JOSA B* **29**, 2581 (2012).
 - [6] J. P. Dowling, Quantum optical metrology—the low-down on high-n00n states, *Contemporary physics* **49**, 125 (2008).
 - [7] K. P. Seshadreesan, P. M. Anisimov, H. Lee, and J. P. Dowling, Parity detection achieves the heisenberg limit in interferometry with coherent mixed with squeezed vacuum light, *New Journal of Physics* **13**, 083026 (2011).
 - [8] C. Lee, J. Huang, H. Deng, H. Dai, and J. Xu, Nonlinear quantum interferometry with bose condensed atoms, *Frontiers of physics* **7**, 109 (2012).
 - [9] S. Ataman, A. Preda, and R. Ionicioiu, Phase sensitivity of a mach-zehnder interferometer with single-intensity and difference-intensity detection, *Phys. Rev. A* **98**, 043856 (2018).
 - [10] J. Jing, C. Liu, Z. Zhou, Z. Ou, and W. Zhang, Realization of a nonlinear interferometer with parametric amplifiers, *Applied Physics Letters* **99** (2011).
 - [11] M. Manceau, F. Khalili, and M. Chekhova, Improving the phase super-sensitivity of squeezing-assisted interferometers by squeeze factor unbalancing, *New Journal of Physics* **19**, 013014 (2017).
 - [12] L.-Y. Hu, C.-P. Wei, J.-H. Huang, and C.-J. Liu, Quantum metrology with fock and even coherent states: Parity detection approaches to the heisenberg limit, *Optics Communications* **323**, 68 (2014).
 - [13] M. Bradshaw, P. K. Lam, and S. M. Assad, Ultimate precision of joint quadrature parameter estimation with a gaussian probe, *Physical Review A* **97**, 012106 (2018).
 - [14] Z. Zhang, C. You, O. S. Magaña-Loaiza, R. Fickler, R. d. J. León-Montiel, J. P. Torres, T. S. Humble, S. Liu, Y. Xia, and Q. Zhuang, Entanglement-based quantum information technology: a tutorial, *Advances in Optics and Photonics* **16**, 60 (2024).
 - [15] K.-H. Luo, M. Santandrea, M. Stefszky, J. Sperling, M. Massaro, A. Ferreri, P. R. Sharapova, H. Herrmann, and C. Silberhorn, Quantum optical coherence: From linear to nonlinear interferometers, *Phys. Rev. A* **104**,

- 043707 (2021).
- [16] W. Du, J. Kong, G. Bao, P. Yang, J. Jia, S. Ming, C.-H. Yuan, J. F. Chen, Z. Y. Ou, M. W. Mitchell, and W. Zhang, *Su(2)-in-su(1,1) nested interferometer for high sensitivity, loss-tolerant quantum metrology*, *Phys. Rev. Lett.* **128**, 033601 (2022).
- [17] M. Manceau, G. Leuchs, F. Khalili, and M. Chekhova, *Detection loss tolerant supersensitive phase measurement with an su(1,1) interferometer*, *Phys. Rev. Lett.* **119**, 223604 (2017).
- [18] J. Xin, *Phase sensitivity enhancement for the su (1, 1) interferometer using photon level operations*, *Optics Express* **29**, 43970 (2021).
- [19] M. Santandrea, K.-H. Luo, M. Stefszky, J. Sperling, H. Herrmann, B. Brecht, and C. Silberhorn, *Lossy su (1, 1) interferometers in the single-photon-pair regime*, *Quantum Science and Technology* **8**, 025020 (2023).
- [20] S. Chang, C. Wei, H. Zhang, Y. Xia, W. Ye, and L. Hu, *Enhanced phase sensitivity with a nonconventional interferometer and nonlinear phase shifter*, *Physics Letters A* **384**, 126755 (2020).
- [21] S. S. Szigeti, R. J. Lewis-Swan, and S. A. Haine, *Pumped-up su(1,1) interferometry*, *Phys. Rev. Lett.* **118**, 150401 (2017).
- [22] Y. Liu, J. Li, L. Cui, N. Huo, S. M. Assad, X. Li, and Z. Ou, *Loss-tolerant quantum dense metrology with su (1, 1) interferometer*, *Optics express* **26**, 27705 (2018).
- [23] J. Tang, J. Li, Y. Cao, Y. Liu, H. Hu, Y. Wang, D. Wu, Z. Deng, H. Yu, X. Wang, *et al.*, *Improvement of phase sensitivity in su (1, 1) interferometer using number-conserving operations*, *Results in Physics* **58**, 107465 (2024).
- [24] D. Li, C.-H. Yuan, Z. Ou, and W. Zhang, *The phase sensitivity of an su (1, 1) interferometer with coherent and squeezed-vacuum light*, *New Journal of Physics* **16**, 073020 (2014).
- [25] Y. Xu, T. Zhao, Q. Kang, C. Liu, L. Hu, and S. Liu, *Phase sensitivity of an su (1, 1) interferometer in photon-loss via photon operations*, *Optics Express* **31**, 8414 (2023).
- [26] C. Lindner, J. Kunz, S. J. Herr, J. Kieβling, S. Wolf, and F. Kühnemann, *High-sensitivity quantum sensing with pump-enhanced spontaneous parametric down-conversion*, *APL Photonics* **8** (2023).
- [27] Z. Ou and X. Li, *Quantum su (1, 1) interferometers: Basic principles and applications*, *APL Photonics* **5** (2020).
- [28] R.-B. Jin, Z.-Q. Zeng, C. You, and C. Yuan, *Quantum interferometers: principles and applications*, *Progress in Quantum Electronics* , 100519 (2024).
- [29] K. A. Kuznetsov, E. I. Malkova, R. V. Zakharov, O. V. Tikhonova, and G. K. Kitaeva, *Nonlinear interference in the strongly nondegenerate regime and schmidt mode analysis*, *Phys. Rev. A* **101**, 053843 (2020).
- [30] F. Roeder, R. Pollmann, M. Stefszky, M. Santandrea, K.-H. Luo, V. Quiring, R. Ricken, C. Eigner, B. Brecht, and C. Silberhorn, *Measurement of ultrashort biphoton correlation times with an integrated two-color broadband su (1, 1)-interferometer*, *PRX Quantum* **5**, 020350 (2024).
- [31] D. A. Kalashnikov, A. V. Paterova, S. P. Kulik, and L. A. Krivitsky, *Infrared spectroscopy with visible light*, *Nature Photonics* **10**, 98 (2016).
- [32] S. K. Lee, T. H. Yoon, and M. Cho, *Interferometric quantum spectroscopy with undetected photons via distinguishability modulation*, *Optics express* **27**, 14853 (2019).
- [33] I. Kviatkovsky, H. M. Chrzanowski, E. G. Avery, H. Bartolomeaus, and S. Ramelow, *Microscopy with undetected photons in the mid-infrared*, *Science Advances* **6**, eabd0264 (2020).
- [34] E. Pearce, N. R. Gemmill, J. Flórez, J. Ding, R. F. Oulton, A. S. Clark, and C. C. Phillips, *Practical quantum imaging with undetected photons*, *Optics Continuum* **2**, 2386 (2023).
- [35] F. Hudelist, J. Kong, C. Liu, J. Jing, Z. Ou, and W. Zhang, *Quantum metrology with parametric amplifier-based photon correlation interferometers*, *Nature communications* **5**, 3049 (2014).
- [36] A. Búzás, E. K. Wolff, M. G. Benedict, P. Ormos, and A. Dér, *Biological microscopy with undetected photons*, *IEEE Access* **8**, 107539 (2020).
- [37] Y. Yang, H. Liang, X. Xu, L. Zhang, S. Zhu, and X.-s. Ma, *Interaction-free, single-pixel quantum imaging with undetected photons*, *npj Quantum Information* **9**, 2 (2023).
- [38] N. R. Gemmill, J. Flórez, E. Pearce, O. Czerwinski, C. C. Phillips, R. F. Oulton, and A. S. Clark, *Loss-compensated and enhanced midinfrared interaction-free sensing with undetected photons*, *Phys. Rev. Appl.* **19**, 054019 (2023).
- [39] G. B. Lemos, V. Borish, G. D. Cole, S. Ramelow, R. Lapkiewicz, and A. Zeilinger, *Quantum imaging with undetected photons*, *Nature* **512**, 409 (2014).
- [40] A. Hochrainer, M. Lahiri, M. Erhard, M. Krenn, and A. Zeilinger, *Quantum indistinguishability by path identity and with undetected photons*, *Rev. Mod. Phys.* **94**, 025007 (2022).
- [41] M. Lahiri, R. Lapkiewicz, G. B. Lemos, and A. Zeilinger, *Theory of quantum imaging with undetected photons*, *Phys. Rev. A* **92**, 013832 (2015).
- [42] A. Vega, E. A. Santos, J. Fuenzalida, M. Gilaberte Basset, T. Pertsch, M. Gräfe, S. Saravi, and F. Setzpfandt, *Fundamental resolution limit of quantum imaging with undetected photons*, *Phys. Rev. Res.* **4**, 033252 (2022).
- [43] B. Viswanathan, G. B. Lemos, and M. Lahiri, *Resolution limit in quantum imaging with undetected photons using position correlations*, *Optics Express* **29**, 38185 (2021).
- [44] I. Kviatkovsky, H. M. Chrzanowski, and S. Ramelow, *Mid-infrared microscopy via position correlations of undetected photons*, *Optics Express* **30**, 5916 (2022).
- [45] S. Töpfer, M. Gilaberte Basset, J. Fuenzalida, F. Steinlechner, J. P. Torres, and M. Gräfe, *Quantum holography with undetected light*, *Science advances* **8**, eabl4301 (2022).
- [46] S. L. Cuozzo, P. J. Barge, N. Prajapati, N. Bhusal, H. Lee, L. Cohen, I. Novikova, and E. E. Mikhailov, *Low-light shadow imaging using quadrature-noise detection with a camera*, *Advanced Quantum Technologies* **5**, 2100147 (2022).
- [47] P. J. Barge, Z. Niu, S. L. Cuozzo, E. E. Mikhailov, I. Novikova, H. Lee, and L. Cohen, *Weak thermal state quadrature-noise shadow imaging*, *Optics Express* **30**, 29401 (2022).
- [48] J. B. Clark, Z. Zhou, Q. Glorieux, A. M. Marino, and P. D. Lett, *Imaging using quantum noise properties of light*, *Optics Express* **20**, 17050 (2012).